

## SPATIAL PROPERTIES OF PRODUCTION FLOW SYSTEM BASED ON RIEMANNIAN MANIFOLD STRUCTURE

KENJI SHIRAI<sup>1</sup>, YOSHINORI AMANO<sup>2</sup>, ATSUYA ANDO<sup>1</sup> AND TAKAYUKI UDA<sup>1</sup>

<sup>1</sup>Faculty of Information Culture  
Niigata University of International and Information Studies  
3-1-1, Mizukino, Nishi-ku, Niigata 950-2292, Japan  
dr.kenji5761@gmail.com; { atsuya; uda }@nuis.ac.jp

<sup>2</sup>Kyohnan Elecs Co., LTD.  
8-48-2, Fukakusanishiura-cho, Fushimi-ku, Kyoto 612-0029, Japan  
y\_amano@kyohnan-elecs.co.jp

Received November 2020; revised March 2021

**ABSTRACT.** *We report that there is a correlation between the probability distribution in production stage and the Fisher information matrix defined in the Riemannian space (hereinafter referred to as FIM). The rationale for this is that, regarding with the process throughput in the probability distribution, it was found that the smaller the trend coefficient is and the larger the variance value is, the more FIM, which is a Riemannian metric, is scattered. Therefore, we present the analysis results of the actual data which is Testrun1 (Test1) through Testrun5 (Test5), obtained in the production flow process. There is no other research that utilizes information geometry for analysis of production processes. It was equal to the results we have reported so far. In other words, logical consistency has been obtained. There is no research specifying the parameters of the dynamic equation defined by a free energy of Ginzburg-Landau (GL) based on real data. Next, we report the change in entropy with regard to volatility. Finally, we report the entropy of three states, that is, a stable state, a state with an assumed phase transition, and a state with a phase transition.*

**Keywords:** Riemannian manifold, Fisher information matrix, Dual flat, Potential energy, Entropy

**1. Introduction.** A motive that the present writers and the like started to promote such kind of research during many years of experience of manufacturing operations of control equipment for general industrial machines is as follows. With respect to Japan after Lehman Shock, Japan's economy has been in a slump, and production bases of manufacturing industries keep moving overseas. Business environments of equipment manufacturing companies in Japanese are extremely severe. In Japan, the situation here is that thorough cost reduction is required. Therefore, we thought that, by finding relation between a company size and a production size of a company, and management parameters mathematically, cost reduction becomes possible.

Regarding research related to the information geometry, there is the report in which, in order to analyze the intrinsic geometrical structure of the manifold of probability distributions, the information geometry was researched [1]. Then, there are still few examples of previous research in stochastic analysis of production processes. In this research, in order to clarify the correlation between the Riemannian metric distribution and the process throughput probability distribution of Testrun1 (Test1) through Testrun5 (Test5) obtained in the production flow system, the information geometry is utilized. Further,

as a result of analysis based on Testrun1 (Test1) through Testrun5 (Test5) collected over 10 years or more from the above-mentioned motive, we have noticed that a correlation between Testrun1 (Test1) through Testrun5 (Test5) data and FIM.

Regarding with our previous research, we have reported on mathematical modeling (deterministic system, stochastic system), optimization, etc. of production processes in small and medium scale [2, 3, 4, 5, 6]. We have constructed the state in which the production density of each process corresponds to the physical propagation of heat [7, 8]. Using this approach, we have shown that the diffusion equation dominates the manufacturing process. In other words, when minimizing the potential of the production field (stochastic field), the equation, which is defined by the production density function  $S_i(x, t)$  and the boundary conditions, is described using the diffusion equation with advection to move in transportation speed  $\rho$ . The boundary conditions mean the closed system in the production field. The adiabatic state in thermodynamics represents the same state [7, 8]. Also, the previous research applying Fluid mechanics that the trial production of a new concept vertical take-off and landing rotorcraft of flexible kite wing attached multicopter is very interesting [9].

Regarding an optimal production capacity, we have reported that the quantity produced is proportional to the rate of return, which aids corporate development and limits production capacity. Therefore, we have employed the Hamilton-Jacobi-Bellman equation to calculate optimal production capacity and determine optimal parameters of the quadratic form evaluation function based on the optimal production capacity [10]. Then, we have investigated a method for optimal control of production processes that include lead-time delays. We have proposed the model that expresses lead-time lag in a strict mathematical model and the model with lead-time delay based on the average regression process, which is the Ornstein-Uhlenbeck process model that is used in mathematical finance. Optimal control is obtained using each state equation [3].

Regarding the analysis of production processes under the Riemannian space, we have reported the mathematical modeling for the production system by utilizing a Riemannian manifold. The production process denotes the diffusion process in the manner similar to that of the physical phenomenon. Based on the theory of constraints (TOC), one method for optimizing the production system is to synchronize the bottlenecks in the system. These bottlenecks may result from worker volatility or from delivery delays caused by other companies. Synchronizing the bottlenecks tends to improve the process throughput. The TOC generally requests the improvement cycle toward the throughput (or lead time); this shortens the bottleneck. However, the TOC does not consider standard physical constraints, which serve as quantitative guidelines for production systems. Specifically, it refers to the following items.

- 1) Reducing the lead time, improving the throughput, and synchronizing the production process by the TOC.
- 2) Sharing the demand information and performing mathematical evaluations.
- 3) Analyzing the reduction and fluctuating demands of the subsystem (using nonlinear vibration theory).
- 4) Basing the inventory management approach on stochastic demand.

In our previous study, we have reported a throughput model for a production flow system using the Riemannian manifold, which is easier to implement than stochastic modeling methods. This model is derived from the stochastic throughput model for producing the propagation necessary to measure synchronization. We have also introduced the Fisher information matrix to specify volatility. To validate the new method and clarify the synchronization processes, we perform a dynamic simulation of the production

system. We have also presented the real synchronous and asynchronous data obtained from the production flow process.

In our present research, the geometric structure of the production space which is composed of the production stages and the workers, should be described. The discussion proceed by regarding the production space as the Riemannian space. The research theme reports that there is some relationship between the probability distribution of each production stage existing in the production space and FIM. When the dispersion of the production process is large, the scattered FIM is larger than when the dispersion is small. This suggests that there is the correlation between the probability distribution at each stage and FIM.

Moreover, we attempt to analyze the phase transition mechanism in the manufacturing industry by treating manufacturing processes as the closed process when seen as the single manufacturing process, that is, the process on which external forces do not act. We instead define order parameters within the manufacturing process and further introduce the Ginzburg-Landau (GL) free energy [11, 12]. The rate of return considerably varies in response to stochastic external forces. For example, considerable delays may arise in the production process or in areas such as logistics. When analyzed by the GL potential energy, the rate of return is influenced by logistical delays and lead times. Here, we analyze the parameters of the potential function using the GL free energy. The rate of return was calculated from the estimates of production orders from September 2014 to September 2016. The parameters of the dynamic equation were empirically obtained from the rate of return data. By specifying these parameters, the potential function and the entropy of the three states could be obtained. The state of a real production process could be specified. We also report the change in entropy with regard to volatility.

The subjects of this paper are as follows. We clarify a correlation between the probability distribution in production stage and the Fisher information matrix defined in the Riemannian space. Furthermore, as a matter not mentioned in the TOC, production delays due to distribution delays are analyzed by utilizing GL potential energy. Finally, we report the entropy of three states: the stable state, the state with the assumed phase transition, and the state with the phase transition.

## 2. Production Business of a Small-to-Midsize Firm.

**2.1. Production systems in the production equipment industry.** We refer to the production system in manufacturing equipment industry studied in this paper. This is not a special system, but “Make-to-order system with version control”. Make-to-order system is a system which allows necessary manufacturing after taking orders from clients, resulting in “volatility” according to its delivery date and lead time. In addition, “volatility” occurs in lead time depending on the contents of make-to-order products (production equipment).

However, effective utilization of the production forecast information on the orders may suppress certain amount of “variation”, but the complete suppression of variation will be difficult. In other words, “volatility” in monthly cash flow occurs and of course influences a rate of return in these companies. Production management systems, suitable for the separate make-to-order system which is managed by numbers assigned to each product upon order, is called as “product number management system” and is widely used.

All productions are controlled with numbered products and instructions are given for each numbered product.

Thus, ordering design, logistics and suppliers are conducted for each manufacturer’s serial numbers in most cases except for semifinished products (unit incorporated into the final product) and strategic stocks.

Therefore, careful management of the lead time or production date may not suppress “volatility” in manufacturing (production).

The company in this study is the “supplier” in Figure 1 and “factory” here. Companies are under the assumption that there are  $N$  (numbers of) suppliers; however, this study deals with one company because no data is published for the rest of the companies ( $N - 1$ ).

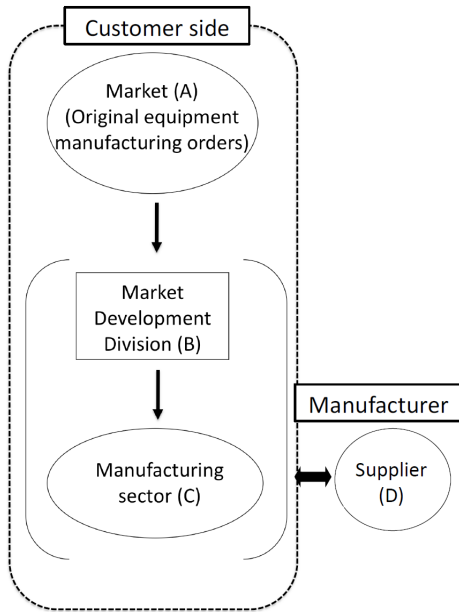


FIGURE 1. Business structure of company of research target

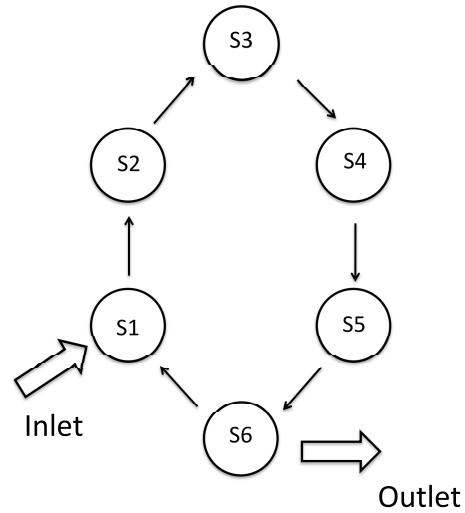


FIGURE 2. Production flow process

**2.2. Production flow system.** A manufacturing process that is termed as a production flow process is shown in Figure 2. The production flow processes, which manufacture low volumes of a wide variety of products, are produced through several stages in the production process. In Figure 2, the processes consist of six stages. In each step S1-S6 of the manufacturing process, materials are being produced by one worker of each step S1 through S6. S1-S6, which are given by Tables 5, 7, 9 and 11 in Appendix A, correspond to the process in Figure 2. The throughput will vary greatly depending on the proficiency level of the worker (Testrun1 through Testrun3-2 in Appendix A).

The direction of the arrow represents the direction of the production flow. In this system, production materials are supplied from the inlet and the end product will be shipped from the outlet.

**Assumption 2.1.** *The production structure is nonlinear.*

**Assumption 2.2.** *The production structure is a closed structure; that is, the production is driven by a cyclic system (production flow system).*

- Reasonability of Assumption 2.1. Assumption 2.1 indicates that the determination of the production structure is considered a major factor, which includes the generation value of production or the rate of return generation structure in a stochastic manufacturing process (hereafter called the manufacturing field). Because such a structure is at least dependent on the demand, it is considered to have a nonlinear structure. Because the value of such a product depends on the rate of return, its production structure is nonlinear. Therefore, Assumption 2.1 reflects the realistic production structure and is somewhat valid.

- Reasonability of Assumption 2.2. Assumption 2.2 is completed in each step and flows from the next step until stage S6 is completed. Assumption 2.2 is reasonable because new production starts from S1. For a more detailed analysis, please refer to our Appendix A.

3. Geometric Structure of Production Field.

3.1. Fisher information matrix in Riemannian space on the production process.

The probability distribution of production stages in the production field is as shown in Figure 3.  $S \in [S_1, S_2, \dots, S_n]$  is the throughput.  $[Q]$  is the production field.

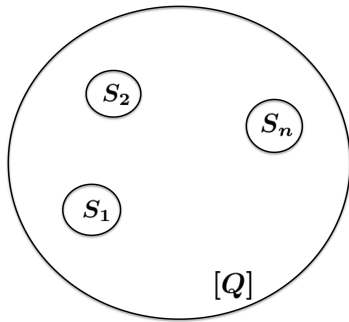


FIGURE 3. Probability distribution of production stages in the production field

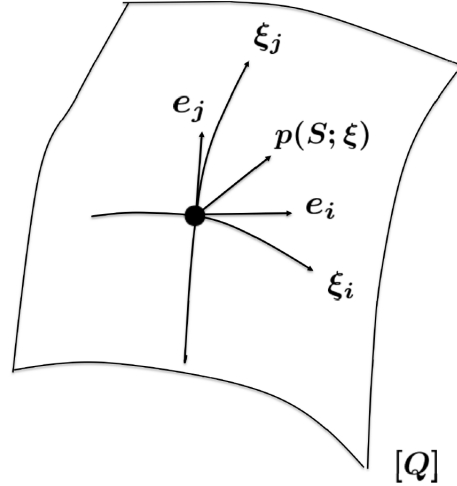


FIGURE 4. Production density of each process in Riemannian space

**Definition 3.1.** Gauss probability density function  $p_i(S_i; \mu_i, \sigma_i)$  of mean  $\mu_i$ , variance  $\sigma_i^2$

$$p_i(S_i; \mu_i, \sigma_i) = \frac{1}{\sqrt{2\pi}\sigma_i} \exp \left\{ -\frac{(S_i - \mu_i)^2}{2\sigma_i^2} \right\} \tag{1}$$

$$S \in \{p_i(S_i; \mu_i, \sigma_i), i = 1, 2, \dots, n\} \tag{2}$$

where Equation (1) indicates uniquely determined given the  $\mu_i$  and the variance  $\sigma_i^2$ .

The production density of each process in Riemannian space is as shown in Figure 4.  $\xi \equiv (\mu, \sigma)$ , the production flow is as follows.

$$d\xi = \sum_{i=1}^n d\xi^i e_i \tag{3}$$

Since we study in the framework of information geometry, we define the Fisher information matrix (Hereinafter referred to as FIM) as follows.

**Definition 3.2.** FIM  $G(\xi)$

$$G(\xi) \equiv (g_{ij}(\xi)) \tag{4}$$

where  $g_{ij}(\xi)$  is derived as follows.

$$\begin{aligned} g_{ij}(\xi) &= \langle e_i, e_j \rangle \equiv E \left( \frac{\partial \ln p_i(S_i; \xi)}{\partial \xi^i} \frac{\partial \ln p_i(S_i; \xi)}{\partial \xi^j} \right), \quad p_i(S_i; \xi) \in A \\ &= \int \frac{\partial \ln p_i(S_i; \xi)}{\partial \xi^i} \frac{\partial \ln p_i(S_i; \xi)}{\partial \xi^j} p_i(S_i; \xi) dS_i \end{aligned} \tag{5}$$

Figure 5 shows that the probability density function can be determined by defining the  $\mu_i$  and the variance  $\sigma_i^2$ . By generalizing this, it is possible to equate a statistical model, which is a family of the following probability distributions, with a manifold, which is a set of parameters that specify the probability distribution. Therefore, the following equation is derived from Equation (1).

$$Q := \{p_i(S_i; \xi) | \xi = (\xi_1, \xi_2, \dots, \xi_n) \in \Xi\} \tag{6}$$

It means that the statistical model  $Q$  put on par with the manifold  $\Xi$  in Equation (6).

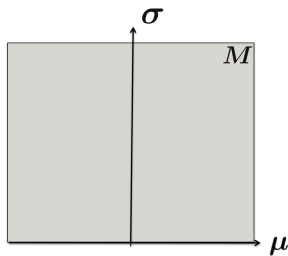


FIGURE 5. Two-dimensional manifold  $M$

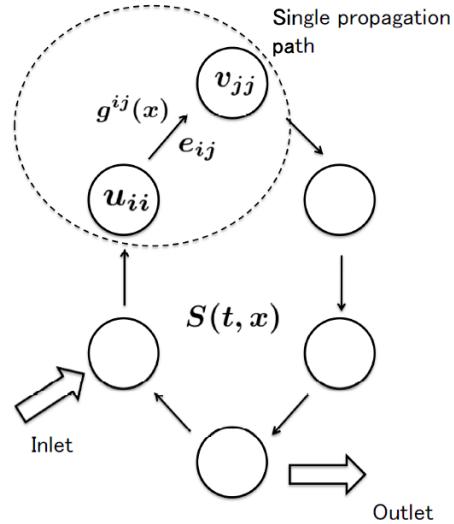


FIGURE 6. Single propagation path of  $u \rightarrow v$

The distance between the probability distributions that exist in each stage in Riemannian space is given by the following equation.

$$ds^2 = \sum_{i,j} g_{ij} d\xi_i d\xi_j \tag{7}$$

where  $g_{ij}$  is FIM.

At this time, the geometry of  $Q$  does not depend on the value of parameter  $\xi$ .

The covariant derivative of  $e_i$  and  $e_j$  is defined as follows.

**Definition 3.3.** Covariant derivative of  $e_i$  in the  $e_j$  direction

$$\nabla_{e_j} e_i = \lim_{d\xi \rightarrow 0} \frac{e'_i - e_i}{d\xi} \tag{8}$$

At this time, the inner product of the covariant derivative is given by the following equation.

$$\Gamma_{i,j,k}(\xi) = \langle \nabla_{e_j} e_i, e_k \rangle \tag{9}$$

where  $\Gamma_{i,j,k}(\xi)$  is also an affine connection coefficient that indicates the connection between production factors which refer to manufactured parts, logistics, and the like.

At this time, the Riemannian connection is defined as follows.

**Definition 3.4.** Riemannian connection  $\Gamma_{i,j,k}(\xi)$

$$\Gamma_{i,j,k}(\xi) = \frac{1}{2} \left( \frac{\partial}{\partial \xi^i} g_{ik} + \frac{\partial}{\partial \xi^j} g_{jk} - \frac{\partial}{\partial \xi^k} g_{ij} \right) = [ij : k] \tag{10}$$

Furthermore, the permissible connection is given by the following equation according to the principle of invariance [1].

$$\Gamma_{i,j,k}^\alpha(\xi) = [ij : k] - \frac{\alpha}{2}\Gamma_{i,j,k} \tag{11}$$

$$\Gamma_{i,j,k} = E \left[ \frac{\partial}{\partial \xi^i} \ln p(S; \xi) \cdot \frac{\partial}{\partial \xi^j} \ln p(S; \xi) \cdot \frac{\partial}{\partial \xi^k} \ln p(S; \xi) \right] \tag{12}$$

where it is limited to the above two equations. It is called  $\alpha$  connection.

Here, let the manifold  $Q$  having  $g$  and  $\nabla$  be  $Q\{S, g, \nabla\}$ . The parallel movement  $\Pi$  of the direction  $d\xi$  of a certain tangent vector to itself is called a geodesic line. It becomes like the following equation.

$$\langle a, b \rangle_Q = \langle \Pi_S, \Pi_S b \rangle_T \tag{13}$$

The following equation is obtained in  $\{S, g, \nabla, \nabla^*\}$ . The event that holds in  $Q$  also holds in  $T$  through the operator  $\Pi$ .

$$\langle a, b \rangle_Q = \langle \Pi_S, \Pi_S^* b \rangle_T \tag{14}$$

where  $\nabla$  and  $\nabla^*$  are called dual enemies.

The  $\alpha$  connection and the  $-\alpha$  connection are dual, and when  $\alpha = 1$ , they are called the exponential connection and are given by the following equation.

$$p(S; \xi) = \exp \left[ \sum_i \xi^i k_i(S) - \varphi(\xi) \right] \tag{15}$$

where  $\xi$  is the affine coordinate system. Equation (15) belongs to the exponential family and is dually flat and linear.

**3.2. Evaluation of production flow system using FIM.** We presented the stochastic throughput model in our previous study as [13, 14]

$$\begin{aligned} \partial S(t, x) = & \left[ a(x) \frac{\partial S(t, x)}{\partial x} + D(x) \frac{\partial^2 S(t, x)}{\partial x^2} \right] \partial t \\ & + \sum_{i=1}^N \partial_d^i(x) S(t, x) \partial W_d^i(t, x) + \sum_{k=1}^N \sigma_0^k(x) \partial W_0^k(t, x) \end{aligned} \tag{16}$$

Then, Equation (16) can be rewritten as follows:

$$\partial S(t, x) = \mathcal{L}S(t, x)dt + \sum_{i=1}^N \partial_d^i(x) S(t, x) \partial W_d^i(t, x) + \sum_{k=1}^N \sigma_0^k(x) \partial W_0^k(t, x) \tag{17}$$

where

$$\mathcal{L} \equiv \frac{1}{2} \sum_{i,j=1}^N \alpha^{ij}(x, t) \frac{\partial^2}{\partial x^i \partial x^j} + \sum_{i=1}^N \beta^i(x, t) \frac{\partial}{\partial x^i} \tag{18}$$

Equation (18) indicates an infinitesimal generator under the measure with no risk. When  $\alpha^{ij}(x, t)$  and  $\beta^i(x, t)$  are derived as spatial elements, Equation (18) can be utilized as the stochastic throughput model [13, 15]. Then, we rewrite Equation (18).

$$\mathcal{L} \equiv - \sum_{i,j} g^{ij}(x) \frac{\partial^2}{\partial x^i \partial x^j} - \sum_{ik} \partial_i g^{ii}(x) \frac{\partial}{\partial x^k} \tag{19}$$

where  $[g^{ij}]$  indicates a reverse matrix of Riemannian metrics  $[g_{ij}]$ . We evaluate in 6 processes and 9 workers configured as shown in Figure 7 and Figure 8.

$$\Delta g^{ii} u_{ii} \equiv g^{ii} v_{jj} - g^{ii} u_{ii} \tag{20}$$

$$\begin{aligned}
 \mathcal{L}f(u_{ii}) &= - \sum_{v_{jj} \sim u_{ii}} g^{ii} \{f(v_{jj}) - f(u_{ii})\} - \sum_{e_{ij}} \Delta g^{ii}(u_{ii}) \frac{f(v_{jj}) - f(u_{ii})}{2} \\
 &= - \sum_{v_{jj} \sim u_{ii}} \frac{f(v_{jj}) - f(u_{ii})}{2} \{f(v_{jj}) - f(u_{ii})\} \\
 &= - \sum_{v_{jj} \sim u_{ii}} w_{ij}(u_{ii}, v_{jj}) \{f(v_{jj}) - f(u_{ii})\}
 \end{aligned}
 \tag{21}$$

Here,  $w_{ij}(u_{ii}, v_{jj})$  represents propagation efficiency and is expressed as follows:

$$w_{ij}(u_{ii}, v_{jj}) = \frac{f(v_{jj}) - f(u_{ii})}{2}
 \tag{22}$$

where  $w_{ij}(v_{jj}, u_{ii}) = w_{ij}(u_{ii}, v_{jj}) > 0$ .

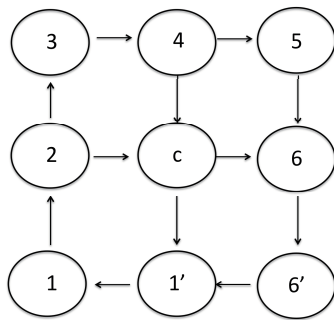


FIGURE 7. Business structure of company of research target

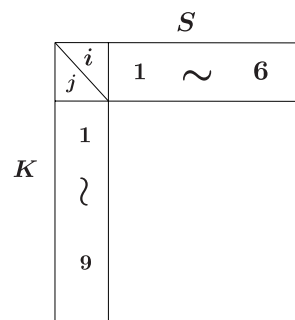


FIGURE 8. Six processes and 9 workers in production flow system in Riemannian space

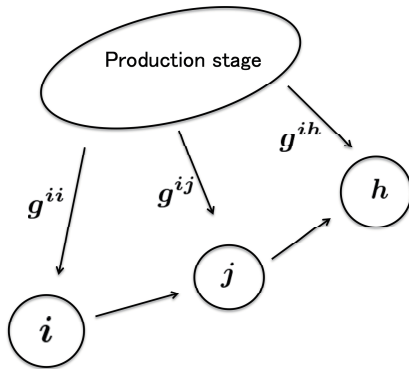


FIGURE 9. Generalized propagation connected in Riemannian space

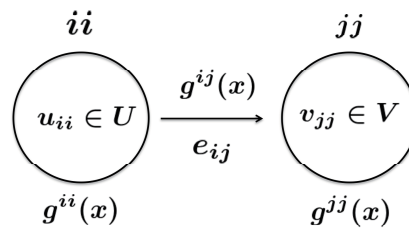


FIGURE 10. Unit propagation path in Riemannian space

Figure 6 shows a single propagation path of  $u \rightarrow v$ , where  $S(t, x)$  represents the propagation characteristics of  $u \rightarrow v$  and is derived as follows:

$$\frac{\partial S(t, x)}{\partial t} = (\text{div grad}_G S)
 \tag{23}$$

Therefore, we obtain as follows. Please refer to our previous research for detailed intermediate calculations [13].

$$\frac{\partial S(t, x)}{\partial t} + v \frac{\partial S(t, x)}{\partial x} = D \frac{\partial^2 S(t, x)}{\partial x^2}
 \tag{24}$$

Equation (24) represents a propagation equation with respect to  $t, x \in V$ , and  $v$  is the weight parameter of the propagation path between each stage in the process.

FIM is a symmetric matrix from Definition 3.2. Furthermore, if the FIM is a definite-value symmetric matrix for any  $G(\xi)$ , the manifold  $\xi \in \Xi$  becomes a Riemannian manifold by introducing a Riemannian metric corresponding to  $G(\xi)$ . The Riemannian metric corresponding to this FIM is called Fisher metric. Therefore, it is possible to measure the distance parameter by introducing Fisher metric given the probability distribution group that is parametrized. The FIM of the Gaussian distribution is as follows

$$\begin{aligned}
 p_i(S_i : \mu_i, \sigma_i) &= \frac{1}{\sqrt{2\pi}\sigma_i} \exp \left\{ -\frac{(S_i - \mu_i)^2}{2\sigma_i^2} \right\} \\
 \ln p_i(S_i : \mu_i, \sigma_i) &= -\ln \sqrt{2\pi} - \ln \sigma_i - \frac{(S_i - \mu_i)^2}{2\sigma_i^2} \\
 \frac{\partial \ln p_i(S_i : \mu_i, \sigma_i)}{\partial \mu} &= \frac{S_i - \mu}{\sigma^2} \\
 \frac{\partial \ln p_i(S_i : \mu_i, \sigma_i)}{\partial \sigma} &= -\frac{1}{\sigma} + \frac{(S_i - \mu)^2}{\sigma^2} \\
 \frac{\partial^2 \ln p_i(S_i : \mu_i, \sigma_i)}{\partial \mu^2} &= -\frac{1}{\sigma^2} \\
 \frac{\partial^2 \ln p_i(S_i : \mu_i, \sigma_i)}{\partial \mu \partial \sigma} &= -2\frac{S_i - \mu}{\sigma^2} \\
 \frac{\partial^2 \ln p_i(S_i : \mu_i, \sigma_i)}{\partial \sigma^2} &= \frac{1}{\sigma^2} - 3\frac{(S_i - \mu)^2}{\sigma^4}
 \end{aligned} \tag{25}$$

Therefore, the FIM of the Gaussian distribution  $G(\xi)$  is as follows.

$$G(\xi) = \frac{1}{\sigma^2} \begin{bmatrix} 1 & 0 \\ 0 & 2 \end{bmatrix} \tag{26}$$

The squared distances of  $\xi$  and  $\xi + d\xi$  using FIM are as follows.

$$ds^2 = [d\mu, d\sigma]G(\xi) \begin{bmatrix} d\mu \\ d\sigma \end{bmatrix} = \frac{(d\mu^2 + 2d\sigma^2)}{\sigma^2} \tag{27}$$

$ds^2$  is inversely proportional to  $\sigma$  in Equation (27). This result is in agreement with previous results [14, 15, 16].

**Definition 3.5.** Connection matrix  $\Gamma_{ij}^k$

$$\Gamma_{ij}^k = \sum_h g^{hk} \Gamma_{ijh} \tag{28}$$

Then we obtain as follows [17]:

$$\partial_i g_{ih} = \Gamma_{ijh}, \quad \partial_i \equiv \frac{\partial}{\partial x^i} \tag{29}$$

For any spatial connection, if  $g^{ij} \cong 0$  in Figure 8, no spatial dual connection is defined. In other words, any stage is isolated from other stages in the production system. The stage is stopped.

Here, the operator  $\mathcal{L}(\bullet)$  in the Riemannian manifold is given by the following equation.

$$\mathcal{L} \equiv - \sum_{i,j} g^{ij} \left( \frac{\partial^2}{\partial x^i \partial x^j} - \sum_k \hat{\Gamma}_{ij}^k \frac{\partial}{\partial x^k} \right) \tag{30}$$

Also,

$$\partial_i g^{ik} = - \sum_{j,h} g^{hk} g^{ij} \left( \hat{\Gamma}_{ijh} + \hat{\Gamma}_{ihj} \right) \quad (31)$$

where  $\hat{\Gamma}_{ijh}$  indicates the Levi-Civita connection matrix [17].

Therefore, we obtain

$$-div_G(grad_G C) = - \sum_{ij} g^{ij} \left( \frac{\partial^2}{\partial x^i \partial x^j} - \sum_k \hat{\Gamma}_{ij}^k \frac{\partial}{\partial x^k} \right) \quad (32)$$

By utilizing information geometry, we presented the probability distribution and production density of each stage of the production process. The potential function  $f(\varphi)$  will be examined in next Section 4.1. Potential in the present research is defined as “ability to create a return”.

When considering like this, we define potential energy (free energy) in a production field as follows [20].

**Definition 3.6.** *Potential energy in production field*

$$\begin{aligned} & [\text{Potential of production field per production density}] \\ &= [\text{Potential for production unit}] + [\text{Fluctuation of potential for production unit}] \end{aligned}$$

Such Definition is almost equivalent to definition of the potential or free energy of a field in physics. We consider that a return is generated by temporal deviation of a potential function (free energy) attributed to a production density function.

**4. Potential Energy and Entropy Analysis of Rate of Return  $h(t)$ .** We describe the phase transition mechanism in the manufacturing industry and the entropy of three states: a stable state, a state with an assumed phase transition, and a state with a phase transition.

**4.1. Potential energy and rate of return of production process.** We report to analyze the phase transition mechanism in the manufacturing industry by treating manufacturing processes as a closed process when seen as a single manufacturing process, that is, a process on which external forces do not act. We instead defined order parameters within a manufacturing process and further introduced the Ginzburg-Landau (GL) free energy.

**4.2. Utilization of Ginzburg-Landau (GL) free energy for production process analysis.**

**Definition 4.1.** *Potential energy function  $f(\varphi)$*

$$f(\varphi) = a_f g(\varphi) + b_g(\varphi) + c_h \{1 - h(\varphi)\} \quad (33)$$

From the relationship between  $\sigma_s$  and  $\sigma$ , we classify as follows.

- 1) as  $\sigma_s = \sigma$ ,  $0 = b_g = c_h$   $T_s = T$
- 2) as  $\sigma_s < \sigma$ ,  $0 = c_h < b_g$   $T_s < T$
- 3) as  $\sigma_s > \sigma$ ,  $0 = c_h > b_g$   $T_s > T$

where  $T_s$  denotes the lead time of the synchronization process (set threshold) and  $T$  denotes the lead time of the actual measurement data.

From the above mentioned description, the overall lead time  $T$  in the case of batch processes is the time taken to produce a piece of equipment in one period of work. Note that only one person produces one piece of equipment in a batch process, and thus,  $T_s = T$ . However, in the case of a production flow system, Item no.1) in the parameter

of Definition 4.1 and Item no.3) in the parameter of Definition 4.1 are not appropriate for determining the throughput. In the case of a batch process, only Item no.2) in the parameter of Definition 4.1 is not appropriate. The lack of sufficient throughput thus leads to increased costs.

Here, the deviation of the lead time is constrained as follows:

$$\frac{\partial f}{\partial t} = -M_\varphi \frac{\delta f(\varphi)}{\delta \varphi} \tag{34}$$

Equation (34) indicates that the lead time deviation (phase deviation) is an equation to move the surface of lead time function. The cause is dependent on the fluctuation of volatility fluctuation.

As a result, we obtain generally as follows:

$$f(\varphi) = a_f g(\varphi) + b_g(\varphi) + c_h \{1 - h(\varphi)\} \tag{35}$$

$$g(\varphi) = \varphi^2(1 - \varphi)^2 \tag{36}$$

$$h(\varphi) = \varphi^2(3 - 2\varphi) \tag{37}$$

GL free energy  $F(\varphi)$  is as follows:

$$F(\varphi) = \int_{\Omega} \left[ \frac{\epsilon^2}{2} |\nabla \varphi|^2 + f(\varphi) \right] dV \tag{38}$$

Then

$$\tau \frac{\partial \varphi}{\partial t} = -\frac{\delta F}{\delta \varphi} \tag{39}$$

By calculation of Equation (39), we obtain as follows:

$$\begin{aligned} \tau \frac{\partial \varphi}{\partial t} &= \epsilon^2 \nabla^2 \varphi + 2a_f^2 \varphi(1 - \varphi) \left\{ \varphi - \frac{1}{2} + \frac{3(c_h - b_g)}{a^2} \right\} \\ &= \epsilon^2 \nabla^2 \varphi + 2a_f^2 \varphi(1 - \varphi) \left\{ \varphi - \frac{1}{2} + \beta \right\}, \quad \beta = \frac{3(c_h - b_g)}{a^2} \end{aligned} \tag{40}$$

Figure 12 illustrates the transition from a lower-energy production process (energy state  $C$ ) to the (higher-energy) next process (energy state  $C'$ ). In Figure 12, the number of production units at each stage of a production unit  $i$  shifts over time. To function effectively, a production process requires a minimum number of personnel. This situation constitutes a shortest path problem. The displacement of the potential in the production field generates a revenue. From the principle of maximum entropy, the entropy increase contributed by the production unit is another source of revenue [5]. We now derive the

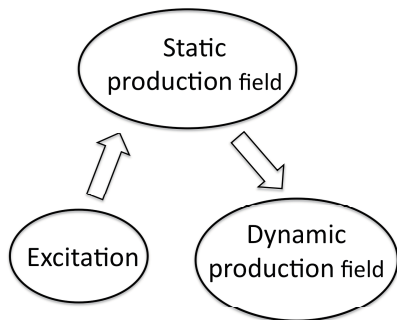


FIGURE 11. Overview of the production field concept

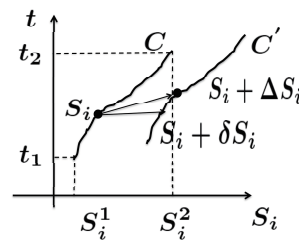


FIGURE 12. Transition from a lower-energy production process to the next process

model equation that constrains the dynamic behavior of the production cost. If the production field sets  $\{S_i(t)\}$ ,  $i = 1, \dots, n$ , introducing sustainable order information and exciting the system with a sustainable target allow the process to progress from a static to a dynamic production field. The free energy of the process is increased by this transition [22]. Please refer more detail information in our previous paper [5]. Here we describe the GL free energy in a manufacturing industry as follows.

**Definition 4.2.** *Free energy:  $F(h)$  related to production quantity*

$$F(h) = \int_0^L \left[ \frac{r}{2} (\nabla h)^2 + W(h) \right] dx \quad (41)$$

Equation (41) indicates that free energy given by the space integration of a function depends on order parameter  $h$  and is GL free energy.  $\nabla h$  represents fluctuations.

From here on,  $h(t, x)$  is the order parameter (rate of return) which depends on almost time only. It is important for the rate of return that a high quality product is completed until planned period. Therefore, we consider the rate of return to  $h(t)$ .

**4.3. Entropy analysis of rate of return  $h(t)$ .** We describe the state equation before discussing entropy.

**Definition 4.3.** *Production density  $C(t, x)$*

$$\frac{\partial C(t, x)}{\partial t} = \mathcal{L}_x C(t, x) \quad (42)$$

where  $t$  and  $x$  denote time and stage number of process. The initial condition and boundary condition are as follows:

$$C(0, x) = C_0(x) \quad (43)$$

$$C(t, x)|_{x \in \partial\Omega} = 0 \quad (44)$$

where  $\partial\Omega$  denotes a start and end process.

Then, we define a stochastic variable for the process time series variable.

**Definition 4.4.** *Stochastic variable  $n(t)$  for the process time series variable*

$$\frac{dn(t)}{dt} = -\nu n(t) + F_R(t) \quad (45)$$

where  $\nu$  and  $F_R(t)$  denote average and exogenous and endogenous disturbances, which are logistics delay, changing delivery date of customer and staff manufacturing mistake, etc.

Here, probability of  $n(t)$  that will enter  $n \sim n + dn$  is as follows: to satisfy the probability that  $n(t)$  falls into  $n \rightarrow n + dn$ , it is to satisfy the following Fokker Planck equation [21]:

$$\frac{\partial P_n(t, n)}{\partial t} = -\nu \frac{\partial P_n(t, n)}{\partial n} + \frac{\partial^2 P_n(t, n)}{\partial n^2} \quad (46)$$

There is no problem even if the Langevin type equation is simplified to a normal probability type differential equation. Langevin type equation can be regarded as a diffusion system [7, 18].

**Assumption 4.1.** *Stochastic differential equation of normal type  $n(t)$*

$$dn(t) = \mu_\xi dt + \sigma_\xi dZ_\xi(t) \quad (47)$$

where  $\mu_\xi$ ,  $\sigma_\xi$  and  $Z_\xi(t)$  are the average, volatility and Wiener process respectively.

**Assumption 4.2.**  $\phi(t)$  denotes a probability density function of normal type with average zero.

$$\phi(t) \equiv \frac{1}{\sqrt{2\pi}\sigma_\xi} \exp\left(-\frac{t^2}{2\sigma_\xi^2}\right) \tag{48}$$

where  $\sigma_\xi$  denotes a volatility.

At the observation time  $t \in [0, T]$ , the probability function  $P(t)$  has the following probability density function in the range  $x \leq n(t) \leq x + dx$  as follows.

**Definition 4.5.** Probability function  $P(t)$

$$P(t) = \int_{-\infty}^t \phi(x)dx \tag{49}$$

Then, we define the entropy as follows.

**Definition 4.6.** Entropy  $S$

$$S = - \int P(t) \ln P(t)dt \tag{50}$$

As  $n(t)$  is the stochastic function, we define the variable  $U$  as follows.

**Definition 4.7.** Stochastic function  $U$

$$U = \langle n(t) \rangle + \xi = n + \xi \tag{51}$$

where  $\langle n(t) \rangle$  and  $\xi$  denote the average  $n$  and white noise respectively [19]. The probability of existence  $P(U > \theta)$  relative to the threshold  $\theta$  is as follows:

$$P(U > \theta) = P(\xi > \theta - n) = P(\xi > \sigma_\xi) \tag{52}$$

Therefore,

$$\begin{aligned} P(\xi > \sigma_\xi) &= \frac{1}{\sqrt{2\pi}\sigma_\xi} \int_{\xi}^{\infty} \exp\left(-\frac{s^2}{2\sigma_\xi^2}\right) ds = \frac{1}{\sqrt{2\pi}} \int_{\xi/\sigma_\xi}^{\infty} \exp\left(-\frac{\alpha^2}{2}\right) d\alpha \\ &= 1 - \Phi(\xi/\sigma_\xi) \end{aligned} \tag{53}$$

where  $\sigma_\xi = \theta - n$ .

Therefore, we obtain from Equations (52) and (53) as follows:

$$P(U > \theta) = 1 - \Phi(\xi/\sigma_\xi) \tag{54}$$

Here, let  $\delta = \xi/\sigma_\xi$ . Then, we obtain as follows:

$$\Phi(\delta) = \frac{1}{\sqrt{2\pi}} \int_{-\infty}^{\delta} \exp\left(-\frac{s^2}{2}\right) ds \tag{55}$$

where  $\sigma_\xi$  denotes the volatility of  $\xi$ .

Then, we define the entropy function for threshold [22]. From Equation (50), we present the numerical calculations in Section 5.

## 5. Numerical Simulation.

**5.1. Numerical results of FIM in the Riemannian space.** Tables 5 to 14 show the productivity (throughput) of each stage (S1-S9) with 6 workers (K1-K6) and 9 stages of work. Recognizing these tables as the production stage space (Riemannian space), we will investigate the relationship between the throughput probability distribution of each stage and FIM. For example, the calculation method of the value 0.322 of Test1-a in Table 1 calculates the FIM from the average variance value 2.49 of the third stage and the fourth

TABLE 1. Analysis result of Testrun1-Testrun5

	$a$	$b$	$c$	$d$	$e$
Test1	0.322	0.180	0.223	0.180	0.07
Test2	4.65	0.727	0.369		
Test3	0.260	0.449	0.727		
Test4	1.34	0.966	0.727		
Test5	1.34	3.38			

TABLE 2. Mean and variance data for each Testrun1 through Testrun5

	$\mu$	$\sigma$
Test1	0.73	0.29
Test2	0.92	0.06
Test3	0.92	0.03
Test4	0.95	0.03
Test5	0.95	0.03

stage of the worker K1 of Testrun1 in Table 6. Table 2 shows the mean and variance values needed to calculate Table 1.

As described above, the connection between stages and the probability distribution are considered. As a result of analyzing the production flow system reported by the author and others, regarding the probability distribution of throughput (lead time), the smaller the trend coefficient ( $\mu$ ) is and the larger the variance value ( $\sigma$ ) is, the more FIM, which is a Riemannian metric, is scattered. Therefore, it was found that there is a correlation between the distribution of the Riemannian metric and the probability distribution.

**5.2. Numerical results of potential function using the phase field method.** The potential energy may change a certain direction according to an external force. The transition of the lead time threshold value mainly depends on the volatility of production processes. Therefore, by setting the volatility of a synchronization process to  $\sigma_s$  and that of a real process to  $\sigma$ , we defined the potential energy function using a phase field method as follows.

Figures 13 to 15 show the potential function graphs at parameter settings of  $a_f$ ,  $b_g$ , and  $c_h$ . The cost calculations on which the rate of return was based used the data of the orders received between September 2014 and December 2014. Figures 16 to 18 show also the graphs obtained from the parameters  $a_f$ ,  $b_g$ , and  $c_h$ . Figures 16 and 17 show that the period before the process improvement can be assumed to contain a potential phase transition. In contrast, Figure 18 shows the period after the process improvement, which is characterized by a stable potential.

The potential function model equations of Figures 13, 14, 15, 16, 17 and 18 are derived as follows (Reprinted above Equations (35), (36) and (37)):

$$\begin{aligned} f(\theta) &= a_f \cdot g(\theta) + b_g \cdot h(\theta) + c_h \cdot (1 - h(\theta)) \\ g(\theta) &\equiv \theta^2(1 - \theta)^2, \text{ Double-well function} \\ h(\theta) &\equiv \theta^2(3 - 2\theta), \text{ Energy density distribution} \end{aligned}$$

In contrast, Figure 18 shows the period after the process improvement, which is characterized by a stable potential.

$$F(\theta) = \int \left[ \frac{r}{2} (\nabla\theta)^2 + W(\theta) \right]$$

$$\varphi^*(\theta, t) \cong \frac{1}{2} \left( 1 - \tanh \left( \frac{\theta - Vt}{2} \right) \right)$$

where  $\theta$  denotes the special solution of following equation.

$$\frac{\partial \theta}{\partial t} = -\tau \frac{\delta F}{\delta \theta}$$

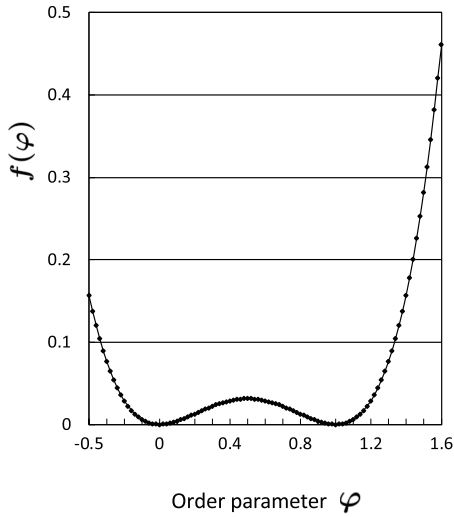


FIGURE 13. Potential function by the phase field method ( $a_f = 0.1, b_g = 0, c_h = 0$ )

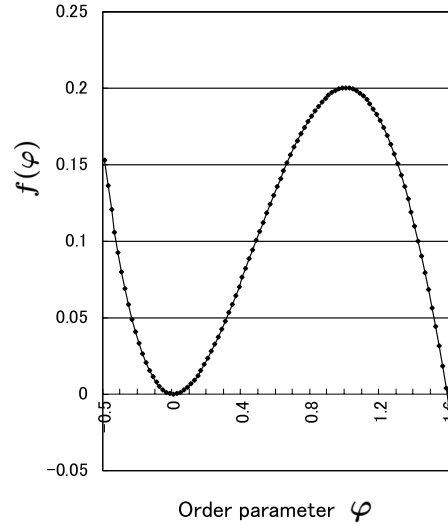


FIGURE 14. Potential function by the phase field method ( $a_f = 0.1, b_g = 0.2, c_h = 0$ )

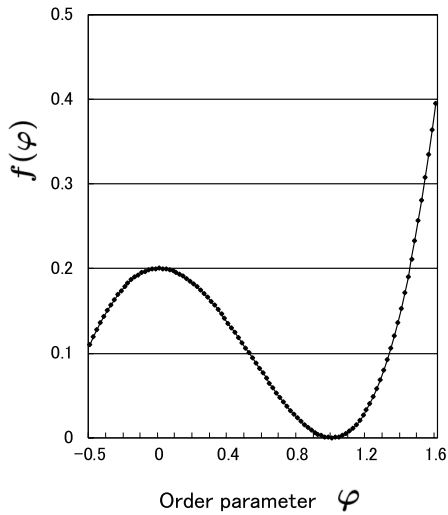


FIGURE 15. Potential function by the phase field method ( $a_f = 0.1, b_g = 0, c_h = 0.2$ )

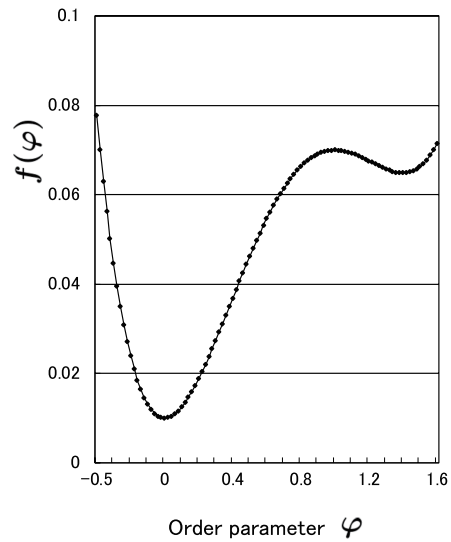


FIGURE 16. Potential function by the phase field method ( $a_f = 0.1, b_g = 0.07, c_h = 0.01$ ):  $\{S_f\}$

In Table 3,  $\{S_f\}$ ,  $\{S_{Local}\}$ , and  $\{S_i\}$  denote the processes before improvement, during improvement  $\{S_f\}$ , and after improvement, respectively.  $\{S_{Local}\} \subset \{S_f\}$  and  $\{S_f\} \rightarrow \{S_i\}$ .

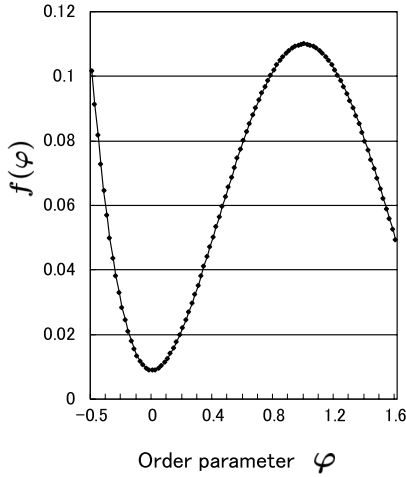


FIGURE 17. Potential function by the phase field method ( $a_f = 0.1, b_g = 0.01, c_h = 0.009$ ):  $\{S_{Local}\}$

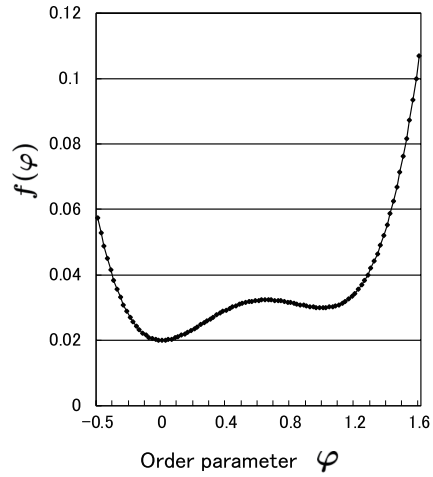


FIGURE 18. Potential function by the phase field method ( $a_f = 0.1, b_g = 0.03, c_h = 0.02$ ):  $\{S_i\}$

TABLE 3. Profit margin before/after improvement of processes

	Before improvement ( $S_{Local}$ )	Current process ( $S_f$ )	After improvement ( $S_i$ )
$\mu$	2.04	6.6	2.02
$\sigma$	3.7	5.3	1.79
Rate of return	0.15 ~ 0.3	-0.1 ~ -0.3	0.2 ~ 0.3

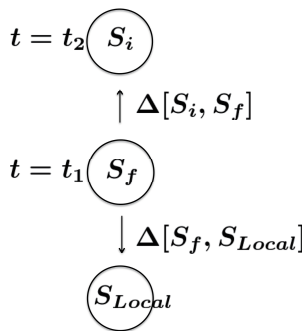


FIGURE 19. Probabilistic representation of process time series

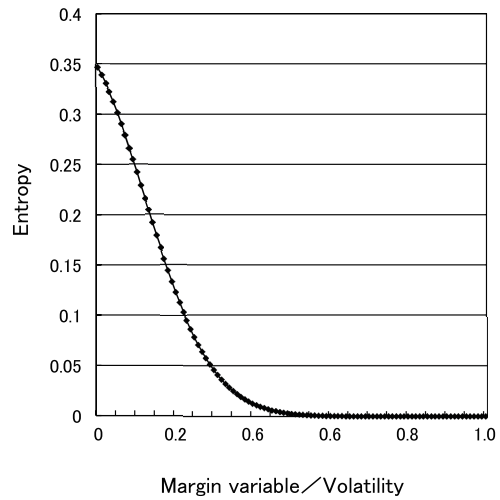


FIGURE 20. Entropy in consideration of standardized volatility  $\{S_i\}$

**5.3. Entropy in consideration of standardized volatility.** Figure 19 shows a process transition diagram derived by applying Equations (58) and (59). Based on Equation (50), Figures 20 to 22 show the entropy values.  $S_i > S_f > S_{Local}$  represents the rate of return. From Figure 19, we define the deviation of entropy as follows.

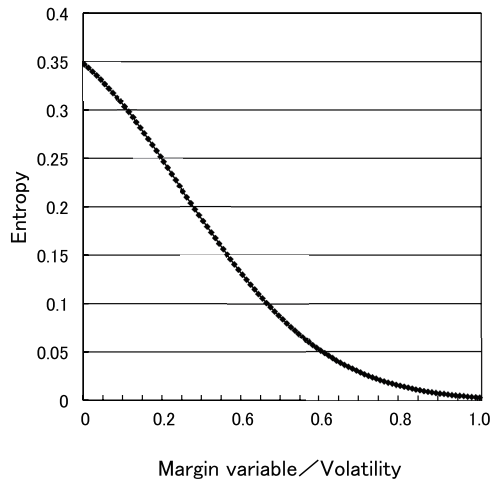


FIGURE 21. Entropy in consideration of standardized volatility  $\{S_f\}$

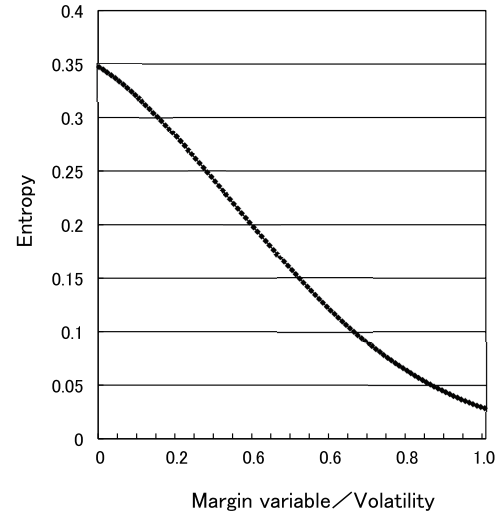


FIGURE 22. Entropy in consideration of standardized volatility  $\{S_{Local}\}$

**Definition 5.1.**

$$\Delta S(t_1, t_2) = S(t_1) - S(t_2) \tag{56}$$

Then,  $S_i$  and  $S_f$  are derived as follows:

$$S_i = S[P_i] + S[\{P_i, P_0\}] \tag{57}$$

$$S_f = S[P_f] + S[\{P_i, P_0\}] \tag{58}$$

$$S_f - S_i = [S[P_f] - S[P_i]] + [S[\{P_i, P_0\}] - S[\{P_f, P_0\}]] = S[P_f] - S[P_i] \tag{59}$$

where  $[S[\{P_i, P_0\}] - S[\{P_f, P_0\}]] = 0$ .

As a result, we obtain as follows:

$$S_f - S_i \cong 6.298 \tag{60}$$

$$S_f - S_{Local} = -4.7572 \tag{61}$$

**6. Conclusion.** We confirmed that the relationship between the probability distribution of each production stage exists in the production space and FIM. In other words, there is the correlation between the probability distribution at each stage and FIM. Then, when analyzed by the GL potential energy, we clarified that the rate of return was influenced by logistical delays and lead times. Regarding with the rate of return data, we presented the actual data which are the estimates of production orders from September 2014 to September 2016. Finally, we reported the entropy of three states: a stable state, a state with an assumed phase transition, and a state with a phase transition.

**REFERENCES**

[1] S. Amari, *Differential-Geometrical Methods in Statistics. Lecture Notes in Statistics*, New York, NY, Springer, 1985.  
 [2] K. Shirai and Y. Amano, Analysis of fluctuations in production processes using Burgers equation, *International Journal of Innovative Computing, Information and Control*, vol.12, no.5, pp.1615-1628, 2016.  
 [3] K. Shirai and Y. Amano, Optimal control of production processes that include lead-time delays, *International Journal of Innovative Computing, Information and Control*, vol.15, no.1, pp.21-37, 2019.

- [4] K. Shirai and Y. Amano, Synchronization analysis of a production process utilizing stochastic resonance, *International Journal of Innovative Computing, Information and Control*, vol.12, no.3, pp.899-914, 2016.
- [5] K. Shirai and Y. Amano, Synchronization analysis of the production process utilizing the phase-field model, *International Journal of Innovative Computing, Information and Control*, vol.12, no.5, pp.1597-1613, 2016.
- [6] K. Shirai and Y. Amano, Model of production system with time delay using stochastic bilinear equation, *Asian Journal of Management Science and Applications*, vol.1, no.1, pp.83-103, 2015.
- [7] K. Shirai and Y. Amano, Production density diffusion equation and production, *IEEJ Trans. Electronics, Information and Systems*, vol.132-C, no.6, pp.983-990, 2012.
- [8] H. Tasaki, *Thermodynamics – A Contemporary Perspective (New Physics Series)*, Baifukan Co., Ltd., 2000.
- [9] K. Hayama and H. Irie, Trial production of kite wing attached multicopter for power saving and long flight, *ICIC Express Letters, Part B: Applications*, vol.10, no.5, pp.405-412, 2019.
- [10] K. Shirai and Y. Amano, Self-similarity of fluctuations for throughput deviations within a production process, *International Journal of Innovative Computing, Information and Control*, vol.10, no.3, pp.1001-1016, 2014.
- [11] K. Shirai and Y. Amano, Parameter setting of a dynamic equation for a production process with phase transition, *International Journal of Innovative Computing, Information and Control*, vol.14, no.4, pp.1495-1509, 2018.
- [12] F. Takase, Multi-mode vibration in the group of transmitters coupled lattice, *KURENAI: Kyoto University Research Information Repository*, vol.413, pp.10-29, 1981.
- [13] K. Shirai and Y. Amano, Use of a Riemannian manifold to improve the throughput of a production flow system, *International Journal of Innovative Computing, Information and Control*, vol.12, no.4, pp.1073-1087, 2016.
- [14] K. Shirai, Y. Amano and S. Omatu, Improving throughput by considering the production process, *International Journal of Innovative Computing, Information and Control*, vol.9, no.12, pp.4917-4930, 2013.
- [15] K. Shirai and Y. Amano, Production throughput evaluation using the Vasicek model, *International Journal of Innovative Computing, Information and Control*, vol.11, no.1, pp.1-17, 2015.
- [16] K. Shirai, Y. Amano and S. Omatu, Propagation of working-time delay in production, *International Journal of Innovative Computing, Information and Control*, vol.10, no.1, pp.169-182, 2014.
- [17] Y. Matsumoto, *Foundation of the Manifold (Basic Math5)*, University of Tokyo Press, 1988.
- [18] K. Shirai and Y. Amano, Characteristic similarity of production key elements greatly affecting profit of a productive business, *International Journal of Innovative Computing, Information and Control*, vol.14, no.5, pp.1929-1946, 2018.
- [19] T. Imamura, *Mathematics in Probability Field*, Iwanami Co., Ltd., 1976.
- [20] K. Shirai, Y. Amano and S. Omatu, Consideration of phase transition mechanisms during production in manufacturing processes, *International Journal of Innovative Computing, Information and Control*, vol.9, no.9, pp.3611-3626, 2013.
- [21] K. Shirai and Y. Amano, Improvement of initial trouble with a certain product group of production processes, *International Journal of Innovative Computing, Information and Control*, vol.14, no.6, pp.2043-2053, 2018.
- [22] K. Kitahara, *Nonequilibrium Statistical Mechanics*, Iwanami Co., Ltd., 2000.

**Appendix A: Analysis of Actual Data in the Production Flow System.** Based on the control equipment, the product can be manufactured in one cycle. The rate of return required to maintain 6 pieces of equipment/day is as follows:

- (Testrun1): Because the throughput of each process (S1-S6) is asynchronous, the overall process throughput is asynchronous. In Table 4, we list the manufacturing time (min) of each process. In Table 6, we list the volatility in each process performed by the workers. Finally, Table 5 lists the target times. The theoretical throughput is obtained as  $3 \times 199 + 2 \times 15 = 627$  (min). In addition, the total working time in stage S3 is 199 (min), which causes a bottleneck. In Figure 23, we plot the measurement

TABLE 4. Correspondence between the table labels and the Testrun number

	Table number	Production process	Working time	Volatility
Testrun1	Table 5	Asynchronous process	627 (min)	0.29
Testrun2	Table 7	Synchronous process	500 (min)	0.06
Testrun3-1	Table 9	“Synchronization with preprocess” method	470 (min)	0.03
Testrun3-2	Table 11	“Synchronization with preprocess” method	470 (min)	0.03

TABLE 5. Testrun1

	WS	S1	S2	S3	S4	S5	S6
K1	15	20	20	25	20	20	20
K2	20	22	21	22	21	19	20
K3	10	20	26	25	22	22	26
K4	20	17	15	19	18	16	18
K5	15	15	20	18	16	15	15
K6	15	15	15	15	15	15	15
K7	15	20	20	30	20	21	20
K8	20	29	33	30	29	32	33
K9	15	14	14	15	14	14	14
Total	145	172	184	199	175	174	181

TABLE 6. Volatility of Table 5

	S1	S2	S3	S4	S5	S6
K1	1.67	1.67	3.33	1.67	1.67	1.67
K2	2.33	2	2.33	2	1.33	1.67
K3	1.67	3.67	3.33	2.33	2.33	3.67
K4	0.67	0	1.33	1	0.33	1
K5	0	1.67	1	0.33	0	0
K6	0	0	0	0	0	0
K7	1.67	1.67	5	1.67	2	1.67
K8	4.67	6	5	4.67	5.67	6
K9	0.33	0.33	0	0.33	0.33	0.33

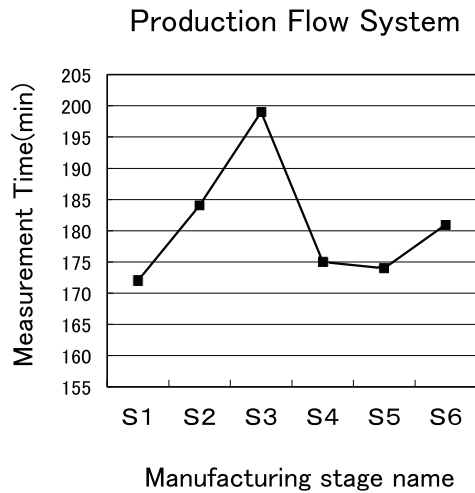


FIGURE 23. Total work time for each stage (S1-S6) in Table 5

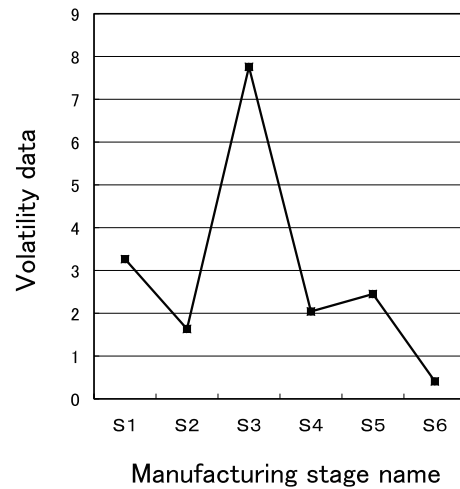


FIGURE 24. Volatility data for each stage (S1-S6) in Table 5

data listed in Table 5, which represents the total working time of each worker (K1-K9). In Figure 24, we plot the data contained in Table 5, which represents the volatility of the working times.

- (Testrun2): Set to synchronously process the throughput. The target time listed in Table 7 is 500 (min), and the theoretical throughput (not including the synchronization idle time) is 400 (min). Table 8 presents the volatility of each working process (S1-S6) for each worker (K1-K9).
- (Testrun3-1): Introduce a preprocess stage. The process throughput is performed synchronously with the reclassification of the process. As shown in Table 9, the theoretical throughput (not including the synchronization idle time) is 400 (min).

TABLE 7. Testrun2

	WS	S1	S2	S3	S4	S5	S6
K1	20	20	24	20	20	20	20
K2	20	20	20	20	20	22	20
K3	20	20	20	20	20	20	20
K4	20	25	25	20	20	20	20
K5	20	20	20	20	20	20	20
K6	20	20	20	20	20	20	20
K7	20	20	20	20	20	20	20
K8	20	27	27	22	23	20	20
K9	20	20	20	20	20	20	20
Total	180	192	196	182	183	182	180

TABLE 8. Volatility of Table 7

	S1	S2	S3	S4	S5	S6
K1	0	1.33	0	0	0	0
K2	0	0	0	0	0.67	0
K3	0	0	0	0	0	0
K4	1.67	1.67	0	0	0	0
K5	0	0	0	0	0	0
K6	0	0	0	0	0	0
K7	0	0	0	0	0	0
K8	2.33	2.33	0.67	1	0	0
K9	0	0	0	0	0	0

TABLE 9. Testrun3-1

	WS	S1	S2	S3	S4	S5	S6
K1	20	18	19	18	20	20	20
K2	20	18	18	18	20	20	20
K3	20	21	21	21	20	20	20
K4	20	13	11	11	20	20	20
K5	20	16	16	17	20	20	20
K6	20	18	18	18	20	20	20
K7	20	14	14	13	20	20	20
K8	20	22	22	20	20	20	20
K9	20	25	25	25	20	20	20
Total	180	165	164	161	180	180	180

TABLE 10. Variance of Table 9

	S1	S2	S3	S4	S5	S6
K1	0.67	0.33	0.67	0	0	0
K2	0.67	0.67	0.67	0	0	0
K3	0.33	0.33	0.33	0	0	0
K4	2.33	3	3	0	0	0
K5	1.33	1.33	1	0	0	0
K6	0.67	0.67	0.67	0	0	0
K7	2	2	2.33	0	0	0
K8	0.67	0.67	0	0	0	0
K9	1.67	1.67	1.67	0	0	0

TABLE 11. Testrun3-2

	WS	S1	S2	S3	S4	S5	S6
K1	20	18	19	18	18	18	18
K2	20	18	18	18	18	18	18
K3	20	21	21	21	21	21	21
K4	16	13	11	11	13	13	13
K5	16	16	16	17	17	16	16
K6	16	18	18	18	18	18	18
K7	20	14	14	13	14	14	13
K8	20	22	22	22	22	22	22
K9	20	25	25	25	25	25	25
Total	168	165	164	163	166	165	164

TABLE 12. Volatility of Table 11, K5: Pre-process

	S1	S2	S3	S4	S5	S6
K1	0.67	0.33	0.67	0.67	0.67	0.67
K2	0.67	0.67	0.67	0.67	0.67	0.67
K3	0.33	0.33	0.33	0.33	0.33	0.33
K4	1	1.67	1.67	1	1	1
K5	0	0	0.33	0.33	0	0
K6	0.67	0.67	0.67	0.67	0.67	0.67
K7	2	2	2.33	2	2	2.33
K8	0.67	0.67	0.67	0.67	0.67	0.67
K9	1.67	1.67	1.67	1.67	1.67	1.67

Table 10 presents the volatility of each working process (S1-S6) for each worker (K1-K9).

- (Testrun3-2): The same as Testrun3-1.

On the basis of these results, the idle time must be set to 100 (min). Moreover, the theoretical target throughput ( $T'_s$ ) can be obtained using the “Synchronization with preprocess” method. This goal is as follows:

$$T_s \sim 20 \times 6 \text{ (First cycle)} + 17 \times 6 \text{ (Second cycle)} \\ + 20 \times 6 \text{ (Third cycle)} + 20 \text{ (Previous process)} + 8 \text{ (Idle-time)}$$

$$\sim 370 \text{ (min)} \tag{62}$$

The full synchronous throughput in one stage (20 min) is

$$T'_s = 3 \times 120 + 40 = 400 \text{ (min)} \tag{63}$$

Using the ‘‘Synchronization with preprocess’’ method, the throughput is reduced by approximately 10%. Therefore, we showed that our proposed ‘‘Synchronization with preprocess’’ method is realistic and can be applied in flow production systems. Below, we represent for a description of the ‘‘Synchronization with preprocess’’.

In Table 13, the working times of the workers K4, K7 show shorter than others. However, the working time shows around target time. Next, we manufactured one piece of equipment in three cycles. To maintain a throughput of six units/day, the production throughput must be as follows:

$$\frac{(60 \times 8 - 28)}{3} \times \frac{1}{6} \simeq 25 \text{ (min)} \tag{64}$$

where the throughput of the preprocess is set to 20 (min). In Equation (64), the value 28 represents the throughput of the preprocess plus the idle time for synchronization. Similarly, the number of processes is 8 and the total number of processes is 9 (8 plus the preprocess). The value of 60 is obtained as 20 (min) × 3 (cycles).

TABLE 13. Total manufacturing time at each stage for each worker, K5: Previous process

	WS	S1	S2	S3	S4	S5	S6
K1	20	18	19	18	18	18	18
K2	20	18	18	18	18	18	18
K3	20	21	21	21	21	21	21
K4	16	13	11	11	13	13	13
K5	16	*	*	*	*	*	*
K6	16	18	18	18	18	18	18
K7	16	14	14	13	14	14	13
K8	20	22	22	22	22	22	22
K9	20	20	20	20	20	20	20
Total	148	144	143	141	144	144	143

TABLE 14. Volatility of Table 13, K5: Previous process

	S1	S2	S3	S4	S5	S6
K1	0.67	0.33	0.67	0.67	0.67	0.67
K2	0.67	0.67	0.67	0.67	0.67	0.67
K3	0.33	0.33	0.33	0.33	0.33	0.33
K4	1	1.67	1.67	1	1	1
K5	*	*	*	*	*	*
K6	0.67	0.67	0.67	0.67	0.67	0.67
K7	0.67	0.67	1	0.67	0.67	1
K8	0.67	0.67	0.67	0.67	0.67	0.67
K9	0	0	0	0	0	0

In Table 4, Testrun3/run4 indicates a best value for the throughput in the three types of theoretical working time. Testrun2 is ideal production method. However, because it is difficult for talented worker, Testrun3/run4 is a realistic method.

In Table 9 and Table 11, Testrun3-1/Testrun3-2 indicate a best value for the throughput in the three types of theoretical working time. Testrun2 is ideal production method. However, because it is difficult for talented worker, Testrun3-1/Testrun3-2 is a realistic method.

The results are as follows. Here, the trend coefficient, which is the actual number of pieces of equipment/the target number of equipment, represents a factor that indicates the degree of the number of pieces of manufacturing equipment.

Testrun1: 4.4 (pieces of equipment)/6 (pieces of equipment) = 0.73,

Testrun2: 5.5 (pieces of equipment)/6 (pieces of equipment) = 0.92,

Testrun3-1 and Testrun3-2: 5.7 (pieces of equipment)/6 (pieces of equipment) = 0.95.

Volatility data represent the average value of each Testrun.